

Subgraph Matching over Graph Federation

Ye Yuan[#] Delong Ma[†] Zhenyu Wen[‡] Zhiwei Zhang[#] Guoren Wang[#]

[#]Beijing Institute of Technology [†]Northeastern University, China [‡]Zhejiang University of Technology

ABSTRACT

Many real-life applications require processing graph data across heterogeneous sources. In this paper, we define the *graph federation* that indicates that the graph data sources are temporarily federated and offer their data for users. Next, we propose a new framework **FedGraph** to efficiently and effectively perform subgraph matching, which is a crucial application in graph federation. **FedGraph** consists of three phases, including query decomposition, distributed matching, and distributed joining. We also develop new efficient approximation algorithms and apply them in each phase to attack the NP-hard problem. The evaluations are conducted in a real test bed using both real-life and synthetic graph datasets. **FedGraph** outperforms the state-of-the-art methods, reducing the execution time and communication cost by $37.3 \times$ and $61.8 \times$, respectively.

1 INTRODUCTION

Graph data (e.g., web graphs, social graphs, knowledge graphs, and biological graphs) are widely used in many applications across various domains, including bioinformatics, finance, and healthcare. The development of big data increases the demand for processing (or analyzing) graph data over several sources with various domains, formats, and query interfaces. In this paper, we name this new computational paradigm *graph federation*, and an illustrative example is shown as follows.

Example 1: Financial Graph Federation for Risk Management. The China Banking Regulatory Commission (CBRC) includes thousands of financial institutions that may build their own graphs or networks for internal data management and analysis [40]. However, there are increasing demands for performing analytics across graphs. For example, before lending money to an enterprise, a bank should conduct due diligence for risk assessment. One of the investigations is the *related-party* analysis, which attempts to find the relation patterns among the bank accounts related to this enterprise. The related-party analysis can help identify illegal behaviors such as money laundering by monitoring the complex sequence of banking transfers. The related-party analysis can be formalized as a party query (or subgraph matching) [18]. Figure 2(a) shows that query pattern Q is a set of normal accounts, including the target enterprise’s account. However, if these accounts have a set of suspicious connections, the target enterprise may be involved in money laundering. We aim to identify these suspicious connections (i.e., query patterns) from three independent graphs (G_1 , G_2 and G_3 in Figure 2(b)) provided by different financial institutions of the CBRC for risk assessment. Unfortunately, many entities from these graphs have the same or similar meaning but are represented in semantical differences. As a result, we need a

unified solution to build the connections among the graphs, namely, *financial graph federation*.

Graph federation is not limited to the financial field. Increasingly, enterprises have embraced data lakes. To uniformly analyze heterogeneous data, some state-of-the-art methods (e.g., federated GraphQL [47]) build a knowledge graph for every data source [9, 14, 39]. These knowledge graphs are composed of a *knowledge graph federation*. Moreover, the resource description framework (RDF) graphs in the Linked Data cloud [1] are semantically different and distributed across the world wide web. Therefore, the linked data cloud implies a *RDF graph federation*.

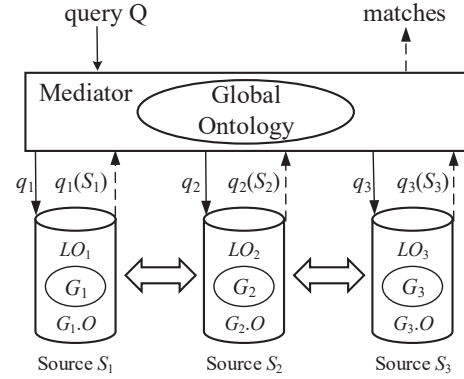


Figure 1: An architecture of graph federation.

These examples indicate that a graph federation GF -based application has a common architecture, as shown in Figure 1. To query a GF , a query Q is submitted to a mediator M . Next, Q is decomposed into a set of subqueries $\{q_1, \dots, q_m\}$ and distributed to a set of n graph sources $\{S_1, \dots, S_n\}$ for data analysis. Every source S_i contains a data graph G_i shared for GF , and the n graphs also make up a *virtual graph* VG (i.e., $VG = \bigcup_{i=1}^n G_i$). S_i also contains a local ontology LO_i and a set of *out-nodes* $G_i.O$, such that each node $v \in G_i.O$ is owned by S_i and other sources S_j ($i \neq j$). Different sources use their out-nodes to communicate with each other. Finally, M aggregates all results collected from S_i and reports to users.

To the best of our knowledge, this is the first paper discussing graph federation applications. As a primary study, we focus on subgraph matching over graph federation in this paper, and a scenario is illustrated in Example 1. Additionally, subgraph matching is one of the most fundamental problems in graph analysis and has many applications, including protein-protein interaction (PPI) networks [23], knowledge bases [56], and program analyses [46, 48].

Subgraph matching has been well studied in traditional graph systems [3, 19, 20, 32, 38, 43], but this is not applicable

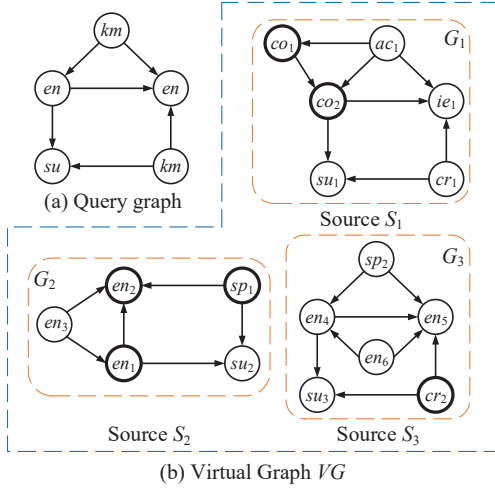


Figure 2: Query and data graphs.

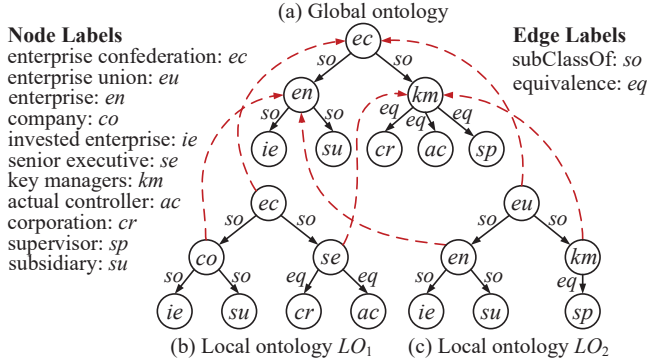


Figure 3: Global and local ontologies.

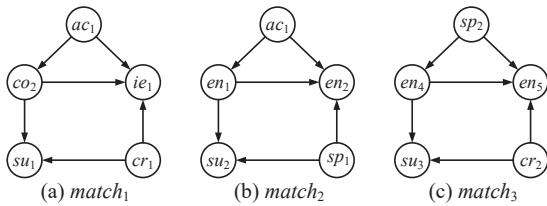


Figure 4: Query answers.

for GF for the following reasons. R1) Traditional subgraph matching requires exact label matching (i.e., the node labels of the source graph and query graph must be the same). As shown in Figure 2, the query graph Q cannot find any matches over the three data graphs G_1 , G_2 and G_3 in this case. For example, node km of Q cannot be mapped to any node by exact label matching. If we recognize that some labels have “equivalence” or “subclass” relations, as shown in Figure 3, Q can find matches m_1 and m_3 from G_1 and G_3 , respectively. However, Q still cannot find a match m_2 across G_1 and G_2 (see Figure 4). This is because different sources have heterogeneous data semantics but may contain the same entities

denoted by the bold nodes in Figure 2. R2) Traditional subgraph matching algorithms [19, 20] are suitable for a single large graph, and some works [3, 32, 38] have been proposed for processing distributed graphs. These works, however, do not consider that in graph federation GF , different sources have varying computational and storage capabilities. A GF is also autonomous: every source provides limited resources to the GF ; e.g., the memory is constrained.

Key idea. To solve R1, we advocate ontology-based subgraph matching (OSM) [57]. Specifically, the mediator M maintains a global ontology GO , and every source keeps a local ontology LO that provides the semantic relationships between the graphs in different sources. The OSM over the GF identifies the matches for Q in the virtual graph VG , where the matches and the query are semantically close according to the GO and LO s. We propose a machine learning approach to build the GO and bridge semantic gaps between the LO s. To tackle R2, we develop efficient approximation algorithms to process an OSM over GF , with theoretical guarantees of the parallel execution time and network overhead. Specifically, we advocate a decomposition-matching-joining method to perform OSM. In the matching, we propose query rewriting based on ontologies to solve the heterogeneous semantics. In the joining, we propose heterogeneity-aware pipelines and scheduling techniques to attack distinct computational and storage capabilities.

Contributions. In summary, we make the following contributions in this paper.

(1) In Section 2, we formally define a graph federation that reflects the features of autonomy and heterogeneity. In this section, we also define OSM over graph federation. (2) In Section 3, we introduce a universal framework to process an OSM over graph federation, i.e., query decomposition, distributed matching and distributed joining. (3) In Section 4.1, we propose the query decomposition algorithm **Dec** and the distributed matching algorithm **Mat**. **Dec** identifies different optimization algorithms to decompose a query Q into a set SQ of star-shaped subqueries. **Mat** progressively generates star matches for the pipeline joining. (4) In Section 5, we develop a distributed joining algorithm that includes logical joining and physical joining. The logical joining applies the pipeline technique to output an efficient corrected joining tree. Based on the joining tree, the physical joining generates and executes an optimized execution plan to minimize the joining process’s parallel execution time and communication cost. (5) In Section 5, we design machine learning algorithms to build the global ontology that bridges the semantic gaps between different graphs. (6) In Section 7, using real-life and synthetic graphs, we experimentally verify the efficiency and scalability of our algorithms.

Position of the work. The graph federation also has dynamic features (i.e., every data graph changes automatically) and private features (i.e., every source may contain sensitive and private data that should be protected). In this paper, however, we concentrate on the features of autonomy, heterogeneous semantics, and different processing capabilities.

We propose novel and systematic solutions to address issues incurred by these features. The dynamic and private features are very different from these features. We will extend our proposed algorithms to solve the issues incurred by the dynamic and private features in other works.

2 PROBLEM DEFINITION

We start with basic concepts of graph federation (Section 2.1) and then formalize the problems of querying graph federation (Section 2.2).

2.1 Basic Concepts

Data graph. We consider labeled, directed, attributed graphs, defined as $G = (V, E, L, F_A)$, where (1) V is a finite set of nodes and $E \subseteq V \times V$ is a set of edges. For each node $v \in V$ (resp. edge $e \in E$) $L(v)$ (resp. $L(e)$) is a *type* (resp. relation) from a finite alphabet. The value of each node v is denoted as $v.val$. $v.val$ is an example of an *attribute* of v , describing a node property. For each node v , its attributes $A_i \in A$, $i \in [1, n]$ are captured in its *property tuple*, $F_A(v)$, defined as a sequence of attribute-value pairs $\{(v.A_1, a_1), \dots, (v.A_n, a_n)\}$. Each pair $(v.A_i, a_i)$ states that the attribute $v.A_i = a_i$.

Graph federation. The integration of distributed graph sources via a central mediator implies a *graph federation* GF . GF consists of a mediator and a set of graph sources. The mediator and graph sources also maintain *ontology graphs* (introduced later). The ontology graphs capture the semantics of different data graphs in sources and can be used to map queries to sources. More specifically, a graph federation needs the following basic components and functionalities:

Graph sources. A collection of n graph sources, or simply sources $GS = \{S_1, \dots, S_n\}$, agree to collectively support query services over their data graphs. Each source S_i manages its own data graph G_i . An S_i also maintains a set of *out-nodes* $G_i.O$, each of which is also a node of G_j in another source S_j . An out-node $v \in G_i.O$ can be owned by multiple sources. In practice, multiple knowledge graphs have the same entity. In Section 6, we introduce how to determine the same out-nodes (e.g., entities) between different data graphs.

In summary, a source S_i maintains the graph G_i as well as the out-node set $G_i.O$. Considering all the sources, a graph federation has a *virtual graph* VG composed of data graphs from every S_i ; i.e., $VG = \bigcup_{i=1}^n G_i$. The virtual graph is physically distributed across n sources. This graph is used to define our problems in the next section.

Figure 2(b) shows three data graphs G_1 , G_2 and G_3 for sources S_1 , S_2 and S_3 , respectively. Every S_i also maintains an out-node set $G_i.O$, denoted by bold circles. For example, S_1 maintains $G_1.O = \{co_1, co_2\}$. To see this, nodes co_1 and co_2 are also maintained in S_2 , represented as en_1 and en_2 ¹. For the same reason, nodes sp_1 and cr_2 are the out-nodes of S_2 and S_3 , respectively.

¹co and en are short for company and enterprise, as shown in Figure 3. co and en refer to the same concept via ontology mapping.

Below, we introduce two features of graph sources, based on which we model the protocols of computation and communication over the graph federation GF .

(1) *Heterogeneous data sizes and semantics.* Different sources build their own data graphs without a uniform standard. Different data graphs thus may have heterogeneous data sizes and semantics. Heterogeneous data semantics refer to those nodes of different data graphs with distinct labels that may refer to the same entity. Ontology-based mapping is an effective mechanism to bridge heterogeneous data semantics [24, 57]. For example, LO_1 and LO_2 (in Figure 3) are the local ontologies of G_1 and G_2 in (Figure 2), respectively. LO_1 and LO_2 form a global ontology GO . There are mappings from LO_1 (or LO_2) to GO , such as $\pi(co) = en$ (represented by the dotted lines in Figure 3), which means they are the same concept but have different names.

Ontology. An ontology graph $O = (V_o, E_o)$ is a directed graph, where V_o is a set of concept labels or attributes and $E_o \subseteq V_o \times V_o$ is a set of semantic relations among the nodes. In practice, an edge $(v, v') \in E_o$ may encode 6 types of relations [30, 36]: (a) *equivalence*, which states that v and v' are semantically equivalent; (b) *hyponym*, which states that v is a kind (or subclass) of v' ; (c) *property*, which states that v is a property of v' in terms of ‘association’ or ‘part-of’ relation; (d) *cause*, which states that v is caused by v' ; (e) *location*, which states that v is a location of v' ; and (f) *temporal*, which states that v is the temporal information of v' .

The relations in an ontology may vary with different domains, but most domain models include the above 6 relations.

A node $u \in V_o$ is a *label ancestor* (resp. *label offspring*) of a node $v \in V_o$ if there is a path from u (resp. v) to v (resp. u) in O with a sequence of “hyponyms” and “equivalences”. Intuitively, u is still a subclass of v if u is a label ancestor of v .

Figure 3(c) shows that nodes km and sp have an equivalent relation and that node en is a subclass of node eu . Additionally, in the figure, node ie is an offspring of node eu , and thus, ie is a subclass of eu .

Every source maintains a local ontology LO_i of G_i . We assume that LO_i contains all the labels of G_i . LO_i can be obtained from G_i by merging nodes with the same type of label, as introduced in the works [59].

The mediator M keeps a global ontology GO of VG . LO_i (resp. GO) can be viewed as a schema that is a summary of the node and edge labels of G_i (resp. VG). For any concept label cl of a LO_i , there is a mapping π from cl to a concept label cl' of GO ; i.e., $\pi(cl) = cl'$. cl and cl' refer to the same concept, although they may have different names. These concepts are generalizations (i.e., superconcepts) of related concepts in local ontologies. In Section 6, we introduce how to compute a global ontology GO from local ontologies. Users can write queries based on GO .

(2) *Heterogeneous computational and storage capabilities.*

Every source S_i is autonomous and manages its data without any interference from other sources. Each S_i voluntarily participates in a graph federation GF by using a *capsule* C_i , which is a logic unit. C_i indicates the shared data graph of S_i . Since each S_i is autonomous and voluntary, it offers limited and various storage and computing resources. We define the resource constraints of each S_i as c_i ; i.e., the consumed memory at every computing time is less than c_i .

2.2 Subgraph Matching

In the following, we first introduce a query graph and then ontology-based subgraph matching.

Query graph. A query graph is a directed graph defined as $Q = (V_q, E_q, L_q, F_q)$, where (1) V_q and E_q are a set of query nodes and query edges, respectively; (2) L_q is a labeling function such that for each node $v \in V_q$ (resp. $e \in E_q$), $L_q(v)$ (resp. $L_q(e)$) is a node (resp. edge) label; and (3) for each node $v \in V_q$, $F_q(v)$ specifies the set $\{A_1, \dots, A_k\}$ of its attributes. Note that $L_q(v)$ or $F_q(v)$ (resp. $L_q(e)$) is a node (resp. edge) label of the global ontology GO . Users can formulate their queries based on GO .

Ontology-based subgraph matching (OSM). Given a query graph $Q = (V_q, E_q, L_q, F_q)$, a data graph $G = (V, E, L, F_A)$ and an ontology O , the OSM finds the subgraphs $G' = (V', E', L', F'_A)$ of G , such that there is a bijective function h from V_q to V where (1) for each node $u \in V_q$, (a) $L(h(u))$ is a label ancestor (or label offspring) of $L_q(u)$ in O , and (b) $F_A(h(u)).A_i$ is a label ancestor (or label offspring) of $F_q(u).A_i$ in O ; and (2) (u, u') is a query edge if and only if $(h(u), h(u'))$ is an edge of G' . We refer to G' as a match of Q in G induced by the mapping h and denote all the matches in G for Q as $Q(G)$.

Problem definition. Given a query graph $Q = (V_q, E_q, L_q, F_q)$ and a graph federation GF with the virtual graph VG , our problem is to find a set of matches $Q(VG)$ of Q in VG via OSM. A match $m \in Q(VG)$ is called a crossing match if m contains nodes in different sources.

Example 2: Figure 4 shows the query answers of OSM Q over the virtual graph VG . We take an example of query node km mapping to the data node ac_1 of G_1 as follows. First, $L'_s(ac_1) = ac$ in LO_1 , and $L_q(km) = km$ in GO . Then, based on the mapping π from LO_1 to GO , $\pi(ac)$ is the child of km in GO , i.e., equivalence. \square

Clearly, subgraph matching over graph federation is an NP-hard problem. This is because its subproblem—subgraph isomorphism—is NP-hard [16]. In the next section, we propose a novel algorithmic framework to address the hard problem.

3 FRAMEWORK OF THE QUERYING ALGORITHM

In this section, we propose a general federated graph querying framework, namely, **FedGraph**, which includes an online phase and an offline phase. The online phase solves the OSM

problem in a decomposition-matching-joining manner, consisting of three steps.

Step 1) Query decomposition. The inputs of **FedGraph** are a graph federation $GF = (M, GS = \{S_1, \dots, S_n\})$ and a query graph Q . Once a Q is submitted to M , a procedure **Dec** is invoked to decompose Q into a set of star queries SQ (detailed in Section 4.1). A star query contains a pivot node and a set of leaves as its neighbors in Q . After query decomposition, SQ is sent to GS for performing distributed matching.

Step 2) Distributed matching. Taking the input from Step 1, **FedGraph** invokes a procedure **Mat** to efficiently generate all matches for each star query in SQ over VG (see Section 4.2). The procedure **Mat** progressively generates the matches, which are fed into the pipeline join in the next step.

Step 3) Distributed joining. The matches produced by **Mat** for multiple star queries are then joined in pipeline parallel by a **Join** procedure to produce complete matches of Q (see Section 5). **Join** includes logical and physical joining, aiming at minimizing the parallel execution time and network overhead. Specifically, logical joining outputs a joining plan that minimizes the time cost. Physical joining executes a joining plan to minimize the traffic cost.

The offline phase of **FedGraph** is the determination of the out-nodes of graph sources and the construction of the ontologies (see Section 6). The online phase needs the out-nodes and ontologies to execute the three steps.

4 QUERY DECOMPOSITION & MATCHING

4.1 Query Decomposition

In this section, we propose an algorithm **Dec** that decomposes a query Q into a set of star subqueries $SQ = \{q_1, \dots, q_m\}$. **Dec** aims to achieve the following two goals.

Goal 1: The number of decomposed star queries should be as small as possible, which intuitively reduces the number of joins.

Goal 2: The number of out-nodes of star matches should be as small as possible, which intuitively reduces the communication costs through these out-nodes.

Achieving goal 1. To achieve goal 1, we have to uncover the following problem: Let Q be a query graph and $SQ = \{q_1, \dots, q_m\}$ be a set of stars such that any edge of Q belongs to only one star $q_i \in SQ$. SQ is called the *star cover* of Q . The problem consists of computing the minimum star cover of Q . It is not difficult to prove that the minimum star cover problem is polynomial equivalent to the minimum node cover problem, which is NP-hard. As a result, our problem is an NP-hard problem.

We leverage the 2-approximate algorithm [51] to construct a star cover from a node cover in polynomial steps, detailed as follows. In every step, we randomly select an edge (a, b) , add a and b to the answer, and remove all edges incident to a or b . This process is repeated until we remove all of the edges.

We can use the same process to create a 2-approximate star cover.

To realize goal 2, **Dec** revises the query decomposition algorithm by picking edges with higher *selectivity* as follows.

Achieving goal 2. We first calculate a selectivity $s(u)$ of a node $u \in Q$. $VG.O$ denotes a set of out-nodes of VG ; i.e., $VG.O = \bigcup_{i=1}^n G_i.O$.

For nodes $u \in Q$ and $v \in VG.O$, $|LO(u)|$ denotes the number of out-nodes v such that $h(u) = v$. We then define the selectivity as $s(u) = \frac{1}{|LO(u)|}$. Intuitively, the larger $s(u)$ is, the smaller the probability of $h(u)$ being an out-node, where h is the mapping of Q to VG (i.e., u and v have an ancestor/descendent relationship in the global ontology).

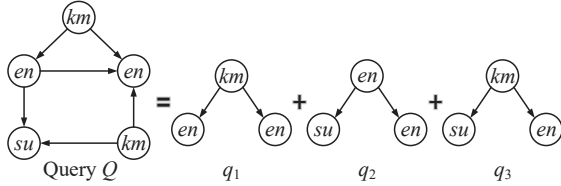


Figure 5: Query decomposition of Q in Figure 2(a).

Figure 6 outlines the detailed steps of **Dec**. **Dec** simulates the process of the approximate algorithm for the node cover problem. Instead of selecting a common edge (u, v) of Q for the node cover, **Dec** picks an edge (u, v) such that $s(u) + s(v)$ is the largest. This difference allows **Dec** to achieve the above two goals.

Algorithm Dec

Input: a query Q .

Output: a set of decomposed star subqueries SQ .

1. initialize $SQ = \phi$; $R = \phi$;
 2. **while** Q has edges **do**
 3. **if** $R = \phi$ **then**
 4. select an edge (u, v) such that $s(u) + s(v)$ is the largest;
 5. **else**
 6. select an edge (u, v) such that $u \in R$ and $s(u) + s(v)$ is the largest
 7. T_u = the stars rooted at u ;
 8. add T_u to SQ ;
 9. $R = R \cup \text{neighbor}(u)$;
 10. remove T_u from Q ;
 11. **if** $\text{deg}(v) > 0$ **then**
 12. T_v = the star rooted at v ;
 13. add T_v to SQ ;
 14. remove all edges in T_v from Q ;
 15. $R = R \cup \text{neighbor}(u)$;
 16. remove u, v and all nodes with degree 0 from R ;
 17. **return** SQ ;
-

Figure 6: Algorithm of query decomposition **Dec**.

Based on the two goals, the query Q in Figure 2(a) can be decomposed into 3 star subqueries with the smallest number of stars and out-nodes, as illustrated in Figure 5.

4.2 Distributed Matching

After query decomposition, we obtain a set of star queries SQ . Our distributed matching scheme aims to maximize the parallelism of the query $q \in SQ$ over all sources $\{S_i\}$. To

Algorithm Mat

Input: a star query q and source S_i .

Output: the match set $q(G_i)$.

1. let u be the pivot node of q ;
 2. **for each** node $l \in V(LO_i)$ **do**
 3. **if** $\text{Reach}(L(u), \pi(L(l)))$ or $\text{Reach}(\pi(L(l)), L(u))$ **then**
 4. let $\text{Cand}(u) = \{v\}$ be the set of nodes of G_i with label $L(l)$;
 5. **if** $\text{Reach}(u, A_i, v, A_i)$ or $\text{Reach}(v, A_i, u, A_i)$
 6. add edges from w to nodes of $q(G_i)$;
 7. **for each** $v \in \text{Cand}(u)$ **do**
 8. **for each** $w \in \text{Neighbor}(v)$ **do**
 9. **for each** leaf node x of q **do**
 10. **if** $\text{Reach}(L(w), \pi(L(x)))$ or $\text{Reach}(\pi(L(x)), L(w))$ **then**
 11. **if** $\text{Reach}(w, A_i, x, A_i)$ or $\text{Reach}(x, A_i, w, A_i)$
 12. add edges from w to nodes of $q(G_i)$;
-

Figure 7: Algorithm of distributed matching **Mat**.

achieve this, the mediator M sends $q \in SQ$ to every source S_i . Every S_i then computes the match set $q(G_i)$ of q in G_i in parallel. Figure 7 shows the detailed steps of **Mat**, where the inputs of **Mat** are a star query q and the source S_i . Its output is the match set $q(G_i)$.

Mat takes the following steps. (1) For the pivot node u of q , **Mat** computes the candidate match set $\text{Cand}(u)$ of u in G_i (lines 1-6). To obtain $\text{Cand}(u)$, **Mat** needs the local ontology LO_i of G_i and the global ontology GO . Recall that a node $l \in LO_i$ has a mapping node $\pi(l)$ in GO and that the label $L(u)$ of u is a node of GO . We thus justify that u matches l if $L(u)$ is an ancestor or offspring of $L(\pi(l))$ in GO (line 3) (the same as for their properties (line 5)). In this case, u may be a subclass or superclass of l . The function $\text{Reach}(L(u), L(v))$ determines such a case. $\text{Reach}()$ speeds up the determination based on a reachability index [53]. (2) Using the same idea, **Mat** calculates the matches of leaf nodes of q (lines 7-12). Once all leaf nodes find their matches, **Mat** returns the match set $q(G_i)$. **Mat** also optimizes this process based on a good match order [55].

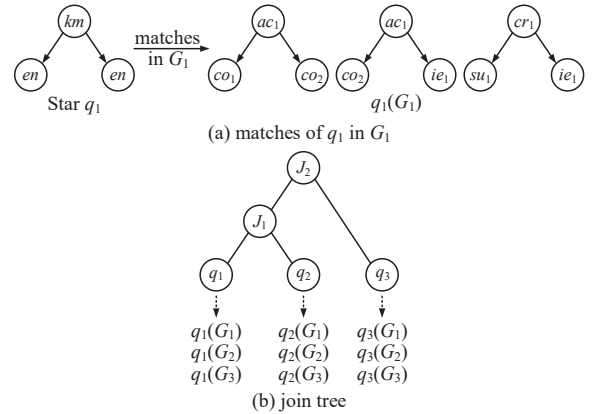


Figure 8: Example of matching and joining tree.

For example, Figure 8(a) shows the matches of star q_1 in G_1 , represented as $q_1(G_1)$. Query Q in Figure 2(a) is decomposed into 3 star subqueries q_1, q_2 and q_3 , as shown in Figure 5. The mediator sends these stars to every source. We aim to obtain all the matches. We use q_1 to match G_1

as an example (see Figure 8(a)). We first identify the node matches ac_1 and cr_1 for the pivot node km . By probing their neighbors, we then find all the matches for the leaf nodes of q_1 (i.e., en). Finally, we have all the matches of q_1 in G_1 , as shown in Figure 8(a).

Note that any node of a star query has only one-hop neighbors in the star. Additionally, a source contains also one-hop neighbor nodes (i.e., out-nodes) of other sources. Therefore, a match $q(G_i)$ is entirely within a source.

5 DISTRIBUTED JOINING

Given Q decomposed to a set of star queries $SQ = \{q_1, \dots, q_m\}$, distributed joining finds all the matches for Q by assembling the matches retrieved by **Mat** on each q_i . We aim to achieve two goals in this section:

- (1) Logical joining. A complete match is constructed from star matches. Logical joining outputs a joining tree that guarantees a corrected joining answer.
- (2) Physical joining. A logical joining plan is executed over graph sources. Physical joining aims at minimizing the parallel execution time and the network overhead.

5.1 Logical Joining

In this section, we develop the algorithm of logical joining **LogJoin** to obtain a complete match of Q . Given a query Q , we decompose it to a set of star queries $SQ = \{q_1, \dots, q_m\}$, denoted $R(q_i)$ as the star matches ($i \in [1, m]$). **LogJoin** computes the set of matches $R(Q)$ as:

$$R(Q) = R(q_1) \bowtie R(q_2) \bowtie \dots \bowtie R(q_m). \quad (1)$$

Joining tree. A join plan determines the order for solving the above joining and processes m rounds of two-way joins. We denote P_i as the i -th partial pattern, whose results are produced in the i th round of the joining plan. Obviously, we have $P_m = Q$. The joining plan is presented in a tree structure, where the leaf nodes are the stars and the internal nodes are the partial patterns. A joining tree T uniquely specifies a joining plan. If all the internal nodes of the joining tree have at least one joining operation as their child, the tree is called a *left-deep tree* [28]. Otherwise, it is a bushy tree [28]. Note that a left-deep tree is a version of bushy tree.

LogJoin advocates the left-deep tree; i.e., **LogJoin** applies a sequence of two-way joins to compute $R(Q)$. This is because a left-deep tree incurs much fewer partitions (i.e., disjoint subtrees) than a bushy tree. This feature allows the following algorithms to be effectively applied to the distributed joining.

Figure 8(b) demonstrates a joining tree T for the three stars in Figure 5. The leaf nodes of T are q_1 , q_2 and q_3 , each of which relates to the star matches.

Optimizing the joining procedure. We use the joining pipeline to perform Equation 1; i.e., we progressively join star matches generated by **Mat**. The pipeline performs joining operations once star matches are generated without waiting for all the matches to be produced. The pipeline technique ensures that the consumed memory of the algorithms in each

source satisfies the storage constraint c_i . We can select a joining order that minimizes the intermediary results of Equation 1. In this paper, we apply the sample-based joining cost estimation method and cost-based joining order selection method [15] to compute an optimal joining order.

5.2 Physical Joining

The previous sections discuss the algorithms used to obtain a logical joining plan; this plan needs to be transferred to a physical joining plan for distributed execution. Given a joining tree T , the physical joining plan aims to maximize the parallel execution and minimize the network overhead of T .

Idea of physical joining. The key idea of physical joining is to optimize the parallel execution and communication costs via *logical scheduling* and *physical scheduling*, respectively.

Logical scheduling partitions T into disjoint subtrees such that these subtrees can be executed in a maximum parallel form. Physical scheduling is an assignment of these subtrees to sources such that the communication cost of executing every subtree is minimized.

Both optimization problems are NP-complete as stated later. To solve the two problems, we propose two polynomial time algorithms with approximation ratio bounds 8ε (ε is a constant) and $\log n$, respectively.

5.2.1 Logical Scheduling. Given a left-deep joining tree T , T has m leaf nodes based on Equation 1. A leaf node of T represents a set of star matches $R(q_i)$ across sources.² These sources can be viewed as a *virtual machine*. Thus, T corresponds to a set of m virtual machines. Logical scheduling is a partitioning of T to m virtual machines such that the parallel execution time of T is *minimized*.

This idea is similar to the classical problem of multiprocessor scheduling with homogeneous environments (i.e., machines with the same computational speeds [22]). However, our environment is heterogeneous, as the m virtual machines have a variety of computing resources. This is because every source has heterogeneous processing capabilities, as introduced in Section 2. In this paper, we propose novel solutions to the heterogeneous scenario. Before introducing our solutions, we first define the following.

We first define a *weighted operator tree* PT originating from the joining tree T . PT shares the same structure with T , i.e., the same nodes and edges of T . The weight t_k of node k is the time to run the operator. The operator is joined if k is an internal node of T , and the operator is matched otherwise. The weight c_{kj} of the edge from node k to node j is the network overhead that both k and j incur for communication if they are scheduled on different virtual machines. The values of t_k and c_{kj} can be obtained by the sample-based cost estimation method for the joining order [15].

Figure 10(a) shows the PT of the joining tree in Figure 8(b). We also need the following definitions.

² $R(q_i)$ might not span all the sources.

Definition 5.1. Given m virtual machines and an operator tree $PT = (V_{pt}, E_{pt})$, a scheduling of PT is a partition of V_{pt} into m sets F_1, \dots, F_m , with set F_k allocated to virtual machine k . The load L_k on the virtual machine k is the cost of executing all nodes in F_k plus the overhead of communicating with nodes on other virtual machines; $L_k = \sum_{i \in F_k} [t_i + \sum_{j \notin F_k} c_{ij}]$.

Every virtual machine has a relative computing speed s_i ($1 \leq i \leq m$). We assume that these speeds have been normalized such that $s_1 = 1$, $s_i \geq 1$ for $2 \leq k \leq m$. The response time of scheduling is $\lambda = \max_{1 \leq k \leq m} \frac{L_k}{s_k}$. The logical scheduling computes a partition of V into F_1, \dots, F_m that minimizes λ . \square

This problem is intractable since the special case in which all edge weights are zero is the NP-complete problem of multiprocessor scheduling [16]. Note that our algorithm (**LogSch**) is not parameterized by s_i ($1 \leq i \leq m$), which is used to analyze only **LogSch**. Therefore, we do not need to estimate the values of s_i .

To schedule a PT , two operations, introduced as follows, are used to modify it:

Definition 5.2. $Collapse(i_1, i_2)$ collapses nodes i_1 and i_2 in tree PT , where i_1 and i_2 are replaced by a new node i . The weight of the new node i is the sum of the weights of the two deleted nodes; i.e., $t_i = t_{i_1} + t_{i_2}$. The edge between i_1 and i_2 is detected if it exists. All other edges connected to either i_1 or i_2 are instead connected to i .

$Cut(i, j)$ modifies a PT by deleting edge (i, j) and adding its weight to that of nodes i and j ; i.e., $t_i^{new} = t_i^{old} + c_{ij}$ and $t_j^{new} = t_j^{old} + c_{ij}$. \square

Now, we propose the logical scheduling algorithm **LogSch**. Figure 9 shows the steps of **LogSch**. **LogSch** consists of two phases: *partitioning* and *the actual scheduling*.

Given an operator tree PT , **LogSch** performs a subprocess **ColCut** (for partitioning, line 1), followed by another subprocess **LPT** (for scheduling, line 2). **LPT** is a classic scheduling algorithm [16]. **LPT** assigns tasks to machines in decreasing order of their processing times. A task is taken from this list and is assigned to a machine whose finishing time is the earliest. **ColCut** partitions PT by iteratively applying $Collapse(i_l, i_2)$ and $Cut(i, j)$ to PT .

As shown in Figure 9, **ColCut** iteratively selects a leaf and decides whether to collapse or cut the edge from the leaf of its parent (line 1). It determines the operation based on the ratio of the leaf weight to the edge weight to its parent. If the ratio is greater than an input parameter α ($\alpha > 1$), it cuts the edge (lines 2-3). If the ratio is less than α , it collapses the leaf to its parent (lines 4-5). This is because the weight of the parent node does not greatly increase. In **ColCut**, a parent node is defined as a node whose child nodes are leaves. In our algorithm, we set the value of α to 3.

Example 3: Figure 10 shows the process of **LogSch** for the PT in Figure 10(a). **LogSch** collapses the leaf node q_1 to its parent J_1 because the new weight of J_1 does not increase substantially. For the same reason, **LogSch** also collapses the leaf node q_3 to its parent J_2 . **LogSch** cuts the edge between

Algorithm LogSch

Input: an operator tree PT , p virtual machines.

Output: a schedule of PT to p virtual machines.

1. invoke **ColCut**(PT) to partition PT into sets F_1, \dots, F_p ;
2. invoke **LPT**() to schedule F_1, \dots, F_p over p virtual machines;

Procedure ColCut(PT)

1. **while** (there exists a parent node m with child j) **do**
 2. **if** ($p_j > \alpha c_{jm}$) **then**
 3. $Cut(j, m)$;
 4. **else**
 5. $Collapse(j, m)$;
-

Figure 9: Algorithm of logical scheduling LogSch.

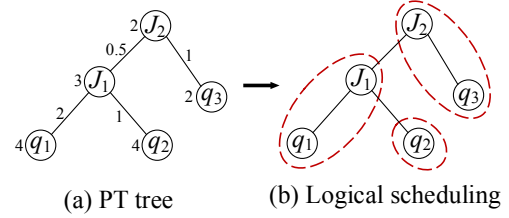


Figure 10: Example of logical scheduling.

the leaf node q_2 and its parent J_1 since this operation does not incur the weight of the resulting partitions. Figure 10(b) gives the final partition of PT . \square

In the following, we apply **LogSch** to the problem in Definition 5.1, for which we prove that **LogSch** provides a constant approximation ratio bound. Here, denote L as the total load; i.e., $L = \sum_{k=1}^p L_k$. The superscript $*$ is used to denote the quantities in the optimal scheduling.

We first have a lemma for a partitioning the ϕ of the PT of the optimal scheduling.

LEMMA 5.3. Suppose that there exists a mapping function f from the fragments produced by partitioning the ϕ of the PT to fragments of the optimal scheduling that satisfies the following conditions: (1) f is total on its domain, and (2) for all F_k ($k \geq 1$) such that $f(F_k) = F_j^*$ ($j \geq 1$), we have $\sum_{L_j^*} \frac{L_k}{L_j^*} \leq r$ ($r > 0$).

After **LPT** is executed for the partitions of ϕ , we have the approximation ratio bound at most $r\varepsilon$, where ε is the ratio bound of **LPT**. \square

Proof. First, we make a schedule Ψ from the optimal schedule. Each fragment F_k of ϕ is assigned to the virtual machine such that $f(F_k)$ has been assigned to the optimal scheduling. Because of totality of f , we can schedule all fragments of ϕ in this manner. From our assumption, if λ_1 is the response time of Ψ , we have $\frac{\lambda_1}{\lambda_1^*} \leq r$. Clearly, if λ_1^* is the response time of the optimal scheduling of fragments produced by ϕ , we have $\lambda_1^* \leq \lambda_1$. Therefore, scheduling these fragments by **LPT** yields a response time of $\lambda \geq \varepsilon \lambda_1$. Then $\frac{\lambda}{\lambda_1^*} \leq r\varepsilon$. \square

THEOREM 5.4. **LogSch** provides an approximation ratio bound of 8ε , where ε is the ratio bound of **LPT**. \square

Proof. We define a relation f from partitions of **ColCut** to those of optimal solution such that $f(F_k) = F_j^*$, if and only

if $\mu(F_k)$ belongs to F_j . Clearly, f is a total function on its domain because each partition of ColCut has one and only one main node and each node of PT belongs to one and only one partition in its optimal solution.

The value of $r = \frac{\sum L_k}{L_j^*}$ such that $\forall k f(F_k) = F_j^*$ is maximized when $\sum L_k$ is maximized and L_j^* is minimized. Assume that f maps p partitions F_1, \dots, F_p to one partition F_j^* . Because of the definition of f , F_j^* must have at least p nodes. F_1, \dots, F_p must be connected because they are mapped into a partition. L_j^* is minimized, if F_j^* cuts all incident edges of the main nodes of F_1, \dots, F_p , except those edges that connect the main nodes to each other. This is because for every edge e_{kj} we have, $c_{kj} < L_k - c_{kj}$. L_j^* is also minimized if F_j^* collapses all edges which connect $\mu(F_1), \dots, \mu(F_p)$ to each other. We therefore have, $\sum_{k=1}^p L_k = \sum_{k=1}^p [m_k + \sum_{j=1}^q t_j + \sum_{l=1}^{\mu} c_l]$, in which m_k is the weight of $\mu(F_k)$, t_j is the weight of the child node j of $\mu(F_k)$ that belongs to F_k and c_l is the weight of the connecting edge between partitions incident $\mu(F_k)$. For each boundary node j of F_k ; we assume that m_j and t_j are the sum of node weights plus the weights of all edges incident to j that are not in F_k .

Because F_1, \dots, F_p form a subtree, and each connecting edge between F_k and F_j is considered for computing the cost of both F_k and F_j , we have, $\sum_{k=1}^p L_k = \sum_{k=1}^p [m_k + \sum_{j=1}^q t_j] + 2 \sum_{l=1}^{p-1} c_l$.

Since connecting edges are cut by ColCut, we have

$$\sum_{k=1}^p L_k < \sum_{k=1}^p [m_k + \sum_{j=1}^q t_j] + \frac{2}{\alpha} \sum_{k=2}^p L_k$$

Let $\alpha > 2$ so

$$\sum_{k=1}^p L_k < \frac{\alpha}{\alpha - 2} \sum_{k=1}^p [m_k + \sum_{j=1}^q t_j]$$

For L_j^* we have, $L_j^* = \sum_{k=1}^p [m_k + \sum_{j=1}^q c_j]$ in which c_j is the weight of the cut edge j incident to $\mu(F_k)$. Note that j cannot be a connecting edge between the main nodes. Since these edges are collapsed by ColCut, we have

$$\begin{aligned} \sum_{k=1}^p L_k &< \sum_{k=1}^p [m_k + \sum_{j=1}^q t_j] + \frac{2}{\alpha} \sum_{k=2}^p L_k \\ \frac{\sum_{k=1}^p L_k}{L_j^*} &< \frac{\sum_{k=1}^p [m_k + \sum_{j=1}^q t_j]}{\sum_{k=1}^p [m_k + \frac{1}{\alpha} \sum_{j=1}^q t_j]} \left(\frac{\alpha}{\alpha - 2} \right) < \frac{\alpha^2}{\alpha - 2} \end{aligned}$$

The above ratio is minimized when $\alpha = 4$, and the minimum value of r is 8. This completes the proof. \square

5.2.2 Physical Scheduling. Consider a joining operation $J = A \bowtie B$ (i.e., an internal node of \mathbf{T}). Since \mathbf{T} is a left-deep tree, pattern A corresponds to partial matches $R(A)$, and pattern B corresponds to star matches $R(B)$. All these matches are distributed over the sources in $MS = \{S_1, \dots, S_n\}$. Physical scheduling studies how to assign $R(A)$ and $R(B)$ to the sources in MS such that the communication cost of executing $A \bowtie B$ is *minimized*. Physical scheduling is performed for every joint node of \mathbf{T} from bottom to top.

The problem is an NP-hard reduction from the distributed joining optimization for relational databases [52]. We thus propose an approximation scheme (PhySch) in this subsection. Specifically, PhySch generates a plan ξ for Q by a reduction from the minimum set cover (MSC) problem [51].

The MSC problem is defined as follows: given a universe set of elements U , X is a collection of weighted sets whose union equals U . We aim to find an X' that covers all elements in U and simultaneously has the minimum total weight of all such subsets of X .

We design PhySch by applying an approximation-preserving reduction [25] from the MSC such that PhySch can optimize the joining overhead by the current approximate algorithms for the MSC.

Reduction. The idea of the reduction is (a) to represent $J = A \bowtie B$ over $R(A) \cup R(B)$ as a cost plan that assigns necessary data movement for answering J and (b) to transform the assignment problem as a variant of the MSC that admits a PTIME logarithmic-factor approximation algorithm [51].

Consider $J = A \bowtie B$ over $R(A) \cup R(B)$, and an instance of MSC is constructed as follows. Given a universe U of elements and a set X of weighted subsets of U , each solution to MSC with an approximation ratio of c encodes a distributed joining plan for J with a cost of at most c -times the minimum cost of all plans for J .

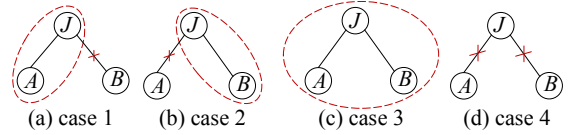


Figure 11: Four cases of physical scheduling.

Four cases from logical scheduling affect PhySch; these cases are introduced as follows. VM is the virtual machine to which logical scheduling assigns a node of PT. I_A is the set of sources making up VM_J ; similarly, for I_B corresponding to B . I_J is the set of candidate sources to which PhySch performs the join J . Figure 11 illustrates the four cases.

- Case 1: J and A are in the same VM , and B is in another VM . Then, $I_J = I_A \setminus I_B$.
- Case 2: J and B are in the same VM , and A is in another VM . Then, $I_J = I_B \setminus I_A$.
- Case 3: J , A and B are in the same VM . Then, $I_J = I_A \cup I_B$.
- Case 4: J , A and B are in different VM s. Then, $I_J = MS \setminus I_A \setminus I_B$.

Case 1 means that the join operation J is executed at the sources in $I_J = I_A \setminus I_B$. The other cases follow the similar meanings.

$R_i(A)$ includes the matches of A at source S_i ($S_i \in I_A$), similar to $R_j(B)$ ($S_j \in I_B$). For any $i, j \in [1, n]$, $u_{ij} = [R_i(A), R_j(B)]$ is called a *unit joining* of J in $R(A) \cup R(B)$. Then:

- (1) U consists of all unit joinings of J in $R(A) \cup R(B)$; and
- (2) X consists of pairs (i, X) for all $i \in [1, n]$ and $X \subseteq U$. We say that (i, X) covers element $u_{jk} = [R_j(A), R_k(B)]$ in U if $u_{jk} \in X$. The weight of (i, X) , denoted by $t(i, X)$, is defined as the sum of the total travel cost of fetching $R_j(A)$ and $R_k(B)$ from sources S_j and S_k to source S_i and the total cost of computing $R_j(A) \bowtie R_k(B)$ for all units $[R_j(A), R_k(B)]$ in X .
- (3) The sources S_i, S_j and S_k obey the rules in the above four cases for $S_i \in I_J, S_j \in I_A$ and $S_k \in I_B$.

Based on the reduction, **PhySch** works as follows: It first initializes a set R to record a set covering the reduced MSC instance. It then iteratively adds set cover (i, X) to R by picking (i_*, X_*) such that the ratio of its weight $t(i_*, X_*)$ to the number of new unit joinings covered by X_* is the minimum of all set covers. After all unit joinings of J are included in R , it interprets R as a set of atomic operations, one for each source, such that for each (i, X) in R and for each $[R_j(A), R_k(B)] \in X$, $R_j(A)$ and $R_k(B)$ are transferred to S_i . Finally, it returns a distributed plan that consists of exactly these atomic operations. It is an $O(\log n)$ -approximation for computing minimum cost joining plans since it is an $O(\log |U|)$ -approximation for the reduced MSC [51], where $|U| = n^2$.

6 LINKING NODES OF GRAPHS

To obtain an out-node of a source, we need to identify the same entity for different graphs. To obtain a global ontology GO , we merge different local ontologies LO by identifying the same concept of different LO s.

To this end, we develop *node linking* that can identify the same node (concept) for two different graphs (resp. ontologies). To obtain the global ontology GO , we apply node linking to every pair of local ontology graphs in the graph federation GF .

General idea. Given two disjoint graphs $G_1 = (V_1, E_1, L_1)$ and $G_2 = (V_2, E_2, L_2)$, node linking computes the common nodes that denote the same entities. Node linking uses these concepts. Given a directed graph G and two nodes u, v in $V(G)$, v is a *child* of u if $(u, v) \in E(G)$; v is a *grandson* of u if there are two consecutive edges from u to v in G ; and v is a *descendant* of u if there is a path from u to v in G .

Node linking has the following intuitive idea. If a node u_0 in G_1 matches a node v_0 in G_2 , the children of u_0 are “similar” to those of v_0 ; the grandsons of u_0 are “similar” to those of v_0 ; and the descendants of u_0 are “similar” to those of v_0 . That is, node linking inductively considers the “similarity” of the descendants of u_0 and the descendants of v_0 .

To define the similarity, we consider a descendant u' of u_0 (resp. v' of v_0) connected by a path ρ_1 (resp. ρ_2). We then define the similarity functions h_v and h_ρ as follows:

$$h_v(u', v') = M_v(L_1(u'), L_2(v')) \quad (2)$$

$$h_\rho(\rho_1, \rho_2) = \frac{M_\rho(\rho_1, \rho_2)}{\text{len}(\rho_1) + \text{len}(\rho_2)} \quad (3)$$

M_v measures the similarity of two vectors of $L_1(u')$ and $L_2(v')$ using a pretrained sentence embedding model [10, 29]; it assesses how similar u' and v' are based on their labels. Different from M_v , M_ρ computes the similarity between two paths ρ_1 and ρ_2 . M_ρ is a bidirectional encoder representation from transformers (BERT) [13]-like function that assesses how similar the association of u' to u_0 and that of v' to v_0 are by treating the labels on paths ρ_1 and ρ_2 as strings.

In practice, we often inspect a certain number of descendants. Thus, we consider the local structural information within k hops of u_0 (resp. v_0) when calculating similarity. $S_k(u)$ is the set of nodes k hops away from u in G . That is, $S_u^k = \{u' | \text{dist}(u, u') \leq k, u' \in V(G)\}$.

Parameters σ and δ are the thresholds for h_v and h_ρ for measuring the similarity of node labels and the associations of labels on paths, respectively.

Node linking. Taking functions (h_v, h_ρ) and thresholds (σ, δ) as parameters, node linking determines whether a pair (u_0, v_0) is a match for nodes $u_0 \in V_1$ and $v_0 \in V_2$.

Given (u_0, v_0) , node linking computes a binary relation $\Pi(u_0, v_0) \subseteq V_1 \times V_2$ that satisfies the following conditions:

- (1) $(u_0, v_0) \in \Pi(u_0, v_0)$; and
- (2) for each pair $(u, v) \in \Pi(u_0, v_0)$, (a) $h_v(u, v) \geq \sigma$, and (b) there exists a set $T_{(u,v)} \subseteq S_{u_0}^k \times S_{v_0}^k$ of pairs (u', v') such that for each $u' \in S_{u_0}^k$, there exists at most one pair (u', v') in $T_{u,v}$; its aggregate score is

$$\sum_{(u', v') \in S_{(u,v)}} h_\rho(\rho_{(u,u')}, \rho_{(v,v')}) \geq \delta;$$

and for each $(u', v') \in T_{(u,v)}$, $(u', v') \in \Pi(u_0, v_0)$. Here, $\rho_{(u,u')}$ is the path selected for u' ; $\rho_{(v,v')}$ is defined similarly. We refer to $S_{(u,v)}$ as a *feature set* of (u, v) .

We say that (u_0, v_0) is a *match* by node linking with $(h_v, h_\rho, \sigma, \delta)$ if there exists a nonempty $\Pi(u_0, v_0)$ satisfying these conditions.

Intuitively, (u_0, v_0) is a match if (1) u_0 and v_0 are similar enough, measured by function h_v based on their labels; (2) there exists a feature set $T_{(u_0, v_0)}$ of pairwise matching pairs such that their associations with (u_0, v_0) are similar enough, measured by the aggregated score with function h_ρ ; and (3) for a pair (u, v) , $S_{(u,v)}$ is a set of pairs (u', v') such that for each important property u' of u , u' finds at most one match v' in $T(u, v)$, and v' is the “best” for u' in terms of h_ρ scores on the paths we select. As a result, (u_0, v_0) is a match if their labels, values and associations are similar enough.

Node and edge models (M_v, M_ρ) . Function $h_v(u, v) = M_v(L_1(u), L_2(u))$ takes two node labels as inputs and returns their semantic similarity. A sentence embedding model [29] is used for $M_v(\cdot, \cdot)$, which takes the string $L_1(u)$ (resp. $L_2(v)$) as input, views it as a sentence, and embeds it as a vector x_u (resp. x_v). Then, the semantic similarity between $L_1(u)$ and $L_2(v)$ is measured by:

$$M_v(L_1(u), L_2(u)) = (|\cos(x_u, x_v)| + \cos(x_u, x_v))/2,$$

where $|\cdot|$ is the absolute value such that $h_v(u, v) \in [0, 1]$.

Similar to M_v , edge model M_ρ takes as input strings $L(\rho_1)$ and $L(\rho_2)$ of the edge labels on the paths and calculates their similarity. Specifically, $L(\rho_1)$ (resp. $L(\rho_2)$) is the input of M_ρ , and its outputs are x_{ρ_1} (resp. x_{ρ_2}). The metric learning model compares x_{ρ_1} and x_{ρ_2} and outputs their similarity score in $[0, 1]$.

Algorithm. We propose the algorithm **NodeLink** to compute the node linking for two graphs. **NodeLink** computes a binary

relation $\Pi(u_0, v_0)$, in which each element $(u, v) \in \Pi(u_0, v_0)$ is a match. Thus, the most important thing of **NodeLink** is to calculate a node match $v \in S_{v_0}^k$ for a given node $u \in S_{u_0}^k$.

Given a node $u \in S_{u_0}^k$, the calculation contains three steps: (1) **NodeLink** computes a candidate node set $Cnd(v) = \{v | h_v(u, v) \geq \sigma, v \in S_{v_0}^k\}$. That is a node set each of which is k hops away from v_0 and has high a high similarity with u . (2) There are possible many paths from u_0 (resp. v_0) to u (resp. v). **NodeLink** ranks these paths by using the path resource allocation algorithm, and returns the top-1 path. Consequently, **NodeLink** obtains one path ρ_u for node u and a path set $PS(v)$ for $Cnd(v)$. (3) **NodeLink** calculates $h_\rho(\rho_u, \rho_v)$ for each $\rho_v \in PS(v)$. Finally, **NodeLink** obtains the match v for u with the largest $h_\rho(\rho_u, \rho_v)$.

The first and third steps are clear. **NodeLink** processes the second step as follows. Given a path $\rho = (u_0, u_1, \dots, u_l)$ ($u_l = u$), **NodeLink** advocates the resource allocation algorithm [35] to compute a measure $R(\rho) = \prod_{i=0}^{l-1} \frac{1}{|ch(v_i)|}$ where $ch(v_i)$ denotes the set of v_i 's children. Intuitively, $R(\rho)$ is a resource that propagates from the starting node u_0 of path ρ , and equally divides at each node in the middle. After resource propagation, $R(\rho)$ quantifies the semantic association of path ρ in terms of the amount of resource that reaches u_l from u_0 via ρ .

More specifically, **NodeLink** is recursive. Given a pair (u, v) of nodes, it finds a feature set $S_{u,v}$ of (u', v') for local descendants u' of u and v' of v , and verifies if (u', v') as a match using the above three steps. For $(u', v') \in S_{u,v}$ that is a match, **NodeLink** sums up the associations between (u, v) and (u', v') , and verifies if the total similarity reaches δ . It returns true if so. Otherwise it backtracks and checks other feature sets. **NodeLink** returns false if there is no feature set that contains a match.

This is nontrivial. (1) When inspecting a pair (u_1, v_1) , it has to select the descendants ($S_{u_1}^k$ and $S_{v_1}^k$) of u_1 and v_1 ; special care has to be taken to avoid picking the same node during different recursive calls. (2) Candidate matches (u_1, v_1) and (u_2, v_2) may depend on each other in, e.g., a strongly connected component. This makes it tricky to backtrack and decide when to return false.

To cope with these we employ two hashmap structures:

(1) *ecache*, to record S_u^k , the descendants selected for each node u , and avoids repeated descendant selection; and

(2) *cache*, to record the current states of candidate matches and dependencies among the candidates. For each pair (u, v) , $cache[u, v]$ is a pair $[\varphi, W]$, which can be either $[false, \varphi]$ or $[true, W]$, where W is a set of candidate matches, and φ is a Boolean value indicating whether (u, v) is confirmed invalid (false) or is valid (true) under the condition that all candidate matches in W are valid.

Observe the following. (a) If (u, v) and (u', v') are interdependent, (u, v) and (u', v') are marked $[true, W_1]$ and $[true, W_2]$ in *cache*, and if $(u', v') \in W_1$ and $(u, v) \in W_2$, then both (u, v) and (u', v') are matches by the definition of node linking. (b) We only need to store matches for nodes of S_u^k

in $cache[u, v]$, i.e., $|W| \leq k$; moreover, the interdependence can be deduced from such W .

In addition, we adopt the following strategies.

(3) For each descendant u' of u we sort the nodes v' in S_u^k in the descending order of the association between (u', v') and (u, v) . When we search a candidate match v' for u' , we follow the order in S_u^k . Intuitively, this helps us decide earlier whether we can get a lineage set with aggregate score at least δ and safely return false, since backtracking in the descending order always yields smaller scores.

(4) When (u, v) is invalidated, we first identify candidates (u', v') that directly depend on (u, v) , i.e., $(u, v) \in cache[u', v']$. We then call **NodeLink** to recheck whether (u', v') is still valid. Observe that this suffices to deal with interdependent candidates; indeed, if (u', v') is also invalid, the candidates that indirectly depend on (u', v') are rechecked when recursive **NodeLink** backtracks.

THEOREM 6.1. *Given graphs (G_1, G_2) and a pair (u_0, v_0) of nodes for $u_0 \in G_1$ and $v_0 \in G_2$, **NodeLink** is correct and takes $O((|V_1| + |E_1|)(|V_2| + |E_2|))$ time to decide whether (u_0, v_0) is a match.*

Proof. For the correctness, it suffices to show the following by induction on recursive calls of **NodeLink**: when **NodeLink** terminates, $cache(u, v) = [true, W]$ if and only if (1) (u, v) and all pairs in W are matches by node linking parameterized with $(h_v, h_\rho, \sigma, \delta)$, and (2) the aggregate score of W is at least δ when $W \neq \Phi$.

For the complexity, (1) it takes at most $O((|V_1| + |E_1|)(|V_2| + |E_2|))$ time to select S_v^k or S_u^k descendants for each pair (u, v) ; and (2) checking whether $(u_0, v_0) \in \Pi(u_0, v_0)$ takes $O(|V_1||V_2|)$ time in the worst case, due to the bound on the number of recursive calls. Here (2) can be verified by representing the computation of **NodeLink** as a tree T and conducting a structure induction on T , while observing the following: (a) there exist at most $O(|V_1||V_2|)$ many candidate matches; (b) for each (u, v) , **NodeLink** is called at most $k^2 + 1$ times, due to the use of hashmap cache; (c) It takes $O(|V_1||V_2|)$ times in total; and (c) during each recursive call, all steps take $O(1)$ time. Therefore, **NodeLink** runs in at most $O((|V_1| + |E_1|)(|V_2| + |E_2|))$ time. \square

7 EVALUATION

We evaluate **FedGraph** using a real test bed with 7 real-life datasets and compare it with 3 baselines. Our highlights are illustrated as follows:

- **FedGraph** is effective at reducing both parallel execution and network cost, outperforming its competitors by 37.3- and 61.8-fold on average, respectively.
- The performance of **FedGraph** is less sensitive with an increasing number of tasks than that of its competitors.
- **FedGraph** has better scalability than its competitors due to the effective techniques for reducing the communication overhead among the sources.
- **NodeLink** of **FedGraph** provides high accuracy graph and ontology integrations.

7.1 Setup

Test bed. FedGraph is deployed on a cluster with 13 machines connected with a high-speed kilomega network, where one machine is selected as the mediator, and the remaining machines are sources. Each machine runs CentOS Linux 7.6 with a 4 Intel Core i7-880 3.06 GHz CPU, 32 GB memory, and 1 TB HDD.

Table 1: Real-life datasets

Dataset	CS	Mater	Engin	Chem	Phy	CrossD	YAGO2
$V(G)$	11.9M	4.6M	5.2M	12.2M	18.1M	27.2M	3.5M
$E(G)$	107.2M	42.2M	36.1M	159.5M	79.5M	51.6M	7.35M
$V(O)$	38	27	53	41	35	103	13
$E(O)$	107	67	189	105	87	856	36
$G_i \cdot O$	15.5K	2.7K	7.1K	2.2K	1.8K	156.8K	78.8K

Real-life dataset. We use 7 real-life property graphs, as shown in Table 1. We first generate five graphs from the Open Academic Graph (OAG) [58] dataset (with 178 million nodes and 2.236 billion edges); these graphs are domain-specific subgraphs from OAG: computer science (CS), materials science (Mater), engineering (Engin), chemistry (Chem), and physics (Phy). We then supplement two widely used graph datasets, CrossDomain (CrossD) [1] and YAGO2 [26]. These property graphs have labels and properties such as papers, authors, venues, and institutes. We use the state-of-the-art scheme [59] to generate an ontology from each data graph. All the statistics of the 7 graphs are listed in Table 1. The global ontology (GO) has 296 nodes and 1357 edges. The GO is very small and is maintained in every source.

Every graph is maintained in a source (machine). Thus, five (i.e., $12-7=5$) sources do not have preloaded graphs. To be more practical for real applications, each source must contain a dataset. We select the 3 largest data graphs and partition each into three subsubgraphs. Every subgraph is distributed to one source, and its ontology is also copied to the corresponding source. Finally, we apply NodeLink to merge the 12 local ontologies into one global ontology that is maintained in the mediator.

Query workload. We first randomly derive star queries from the 7 property graphs. The star queries have labels and properties. We then extend the stars by adding nodes and edges to generate queries with more complex and larger structures, e.g., cliques. We use Q_i to denote the size of a query Q , where i is the number of nodes of Q . For each Q_i , we generate a set of 20 queries and report the average performance. In the experiment, we set the query sets as Q_2 , Q_4 , Q_6 , Q_8 and Q_{10} , where Q_6 is the default set.

Implementation. We develop a prototype system of FedGraph, which employs Neo4j as the database at each source. As we discuss in Section 3, there are three key phases of the FedGraph framework. The algorithms of distributed matching and joining are developed in Neo4j and deployed at each source. The algorithm of query decomposition is developed in the mediator.

To reflect **autonomy**, we partition the 12 sources into 4 groups, i.e., 3 sources in each group. The **heterogeneity**

is reflected in two ways: (1) the memories of the sources belonging to 4 groups are constrained to 50%, 40%, 30% and 20% of their capacities; and (2) the datasets deployed on various sources have different sizes and semantics.

Baselines. We compare FedGraph with the following algorithms.

(1) **Match** is an OSM algorithm for a centralized environment [57]. It follows the filtering-verification strategy, which directly computes matches from the extracted small subgraph without searching the entire graph. To apply it to graph federation, we make the following adaptation. We extract a subgraph from each G_i using **Match**. The subgraph retains the out-nodes of G_i . We then send Q to every S_i to execute **Match**. Note that **Match** may span multiple sources through out-nodes since the matches of Q might span multiple G_i .

(2) **DisRDF** processes subgraph matching over a distributed RDF graph by using a “partial evaluation and assembly” framework [41]. DisRDF cannot support ontology-based matching. To adapt it to graph federation, we feed our matching algorithm (see Figure 7) into the “partial evaluation” phase of DisRDF. During the assembly, DisRDF relies on a straightforward joining strategy that cannot schedule any intermediate computations as FedGraph.

(3) **BinJoin** computes subgraph matching by solving a series of binary joins [31]. It first decomposes the query graph into a set of joined units (e.g., TwinTwig) whose matches can serve as the base relations of the join. BinJoin then joins the base relations based on a near optimal joining order. Similar to DisRDF, BinJoin focuses only on the optimal joining order but neglects the heterogeneity of graph federation.

Metrics. In the experiments, we evaluate the *total execution time* and *communication cost* of the algorithms. The communication cost is measured by the number of exchanged messages, including the messages exchanged between the mediator and the sources, as well as the messages exchanged between the sources.

7.2 Experimental Results

Exp-1: accuracy of the node linking. To evaluate NodeLink, we train the machine models M_v and M_p . NodeLink is executed for every pair of graphs from the 7 datasets, and its quality is evaluated by the F-measure. The F-measure is defined with the precision and recall [7]. Here, the precision, recall and F-measure are (1) the ratio of true matches to matches returned, (2) the ratio of true matches to annotated match pairs in the dataset, and (3) $2 \cdot (\text{precision} \cdot \text{recall}) / (\text{precision} + \text{recall})$, respectively.

We perform our evaluation with three settings: (1) we vary k from 1 to 5 by fixing $\sigma = 0.8$ and $\delta = 2$; (2) we vary σ from 0.5 to 0.9 by fixing $k = 20$ and $\delta = 2$; and (3) we vary δ from 1.0 to 3.0 by fixing $k = 20$ and $\sigma = 0.8$. Table 2 reports the evaluation results of precision (Acc), recall (Rec) and F-measure (f -m).

Table 2: Accuracy of node linking (Exp-1).

$\delta=2 \sigma=0.8$				$\delta=2 k=20$				$k=20 \sigma=0.8$			
k	Acc	Rec	f -m	σ	Acc	Rec	f -m	δ	Acc	Rec	f -m
1	0.61	0.09	0.15	0.5	0.58	0.11	0.17	1	0.64	0.08	0.15
2	0.66	0.24	0.35	0.6	0.6	0.19	0.29	1.5	0.63	0.13	0.21
3	0.72	0.56	0.62	0.7	0.67	0.51	0.58	2	0.73	0.95	0.88
4	0.82	0.98	0.88	0.8	0.75	0.97	0.88	2.5	0.52	0.08	0.11
5	0.91	0.87	0.88	0.9	0.9	0.6	0.72	3	0.43	0.05	0.09

With setting (1), the F-measure first increases and then remains stable after reaching a k of approximately 4. With setting (2), the F-measure first grows steadily when σ increases; it reaches the peak at $\sigma = 0.8$ and then drops sharply with larger σ . The accuracy with setting (3) exhibits a similar trend to that with setting (2). From the evaluation, we observe that the F-measure is the best at $\delta = 2.0$. Therefore, we set the parameters as $\sigma = 0.8$, $\delta = 2$ and $k = 4$ for the following experiments.

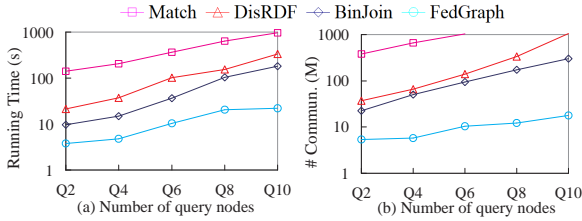


Figure 12: Impact of query sizes (Exp-2).

Exp-2: impact of query sizes. To evaluate the impact of query sizes, we vary the query size from Q2 to Q10 and then apply FedGraph as well as the comparison algorithms.

Figure 12 shows that both execution time and communication cost of Match, DisRDF and BinJoin grow exponentially, while that of FedGraph has less of an upward trend than the others. On average, FedGraph exhibits 107.5, 23.8, and 18.7 times fewer communications than Match, DisRDF and BinJoin, respectively, and is 39.6, 16.5 and 11.2 times faster. Notably, this advantage is more significant with increasing query size. This is because FedGraph optimizes all three phases of the framework instead of the exhaustive search of the compared algorithms and thereby has a lower chance of being stuck in a local optimum.

Figure 13 shows the performance of each phase of FedGraph with respect to query size. Specifically, Figure 13(a) reports the running time of Dec, Mat, LogJoin, LogSch and PhySch, and Figure 13(b) gives the communication cost of the distributed matching (Match) and the distributed joining (Join).

We observe that PhySch dominates most of the running time, followed by LogJoin, LogSch, Mat, and Dec. This result is consistent with our intuition that PhySch tries every feasible joining plan to select the optimal one and that Dec executes only in the local mediator. For communication, Join contributes more than 80% of the traffic of FedGraph, whereas Match incurs less than 20% of that of FedGraph.

Exp-3: impact of source numbers. To evaluate the scalability, we vary the source number from 4 to 12. Figure 14 shows

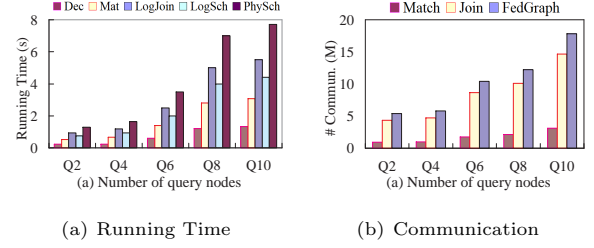


Figure 13: Performance of each phase of FedGraph.

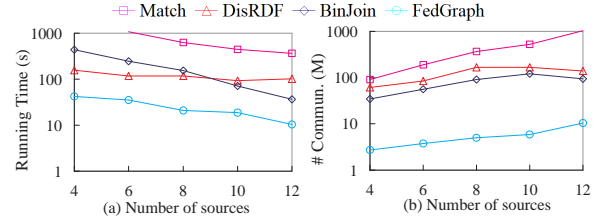


Figure 14: Impact of source numbers (Exp-3).

that FedGraph outperforms other methods in terms of scalability, yielding the minimum execution time and communication cost. In general, all execution times decrease with increasing source number, and adding more sources causes an increase in the communication cost. Because of the source heterogeneity, the decrease in execution time and the increase in communication cost are not completely proportional to the increase in the source number. Moreover, Figure 14(b) shows that FedGraph introduces less network overhead with a varying number of sources than other algorithms; i.e., the growth of the communication cost of FedGraph is much smaller than that of the others with increasing sources.

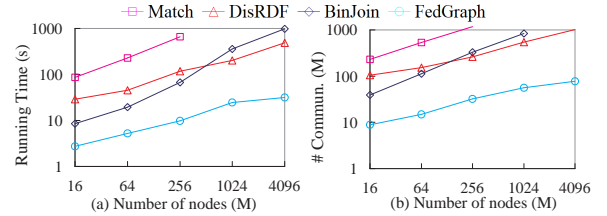


Figure 15: Impact of graph sizes (Exp-4).

Exp-4: impact of graph sizes. Finally, we examine the impact of the data graph size. Here, we use a new experimental setting as follows. We develop a graph generator to randomly produce synthetic graphs; this generator is controlled by three parameters: the number of nodes $|V|$, the number of edges $|E|$, and the size $|L|$ of the node label set. Additionally, we generate ontology graphs for the set of synthetic graphs sharing the same set of labels L , controlled by the same set of parameters. Based on the setting, we generate 5 data graphs and 5 ontology graphs. Every data graph is randomly partitioned and distributed across the 12 sources. NodeLink is used to identify the out-nodes and the global ontology.

We also generate a set of 20 Q6 queries according to L . We report the average results.

Figure 15 presents the experimental results by varying the node numbers of the data graphs from 16M to 4,096M. **FedGraph** consistently performs the best of all the methods. This advantage amplifies as the graph size increases. For example, on average, the execution time of **FedGraph** is $32.5 \times$ less than other algorithms, and it sends 85.3% fewer messages than the other algorithms. **FedGraph** is very efficient; e.g., it takes 30 seconds for the graph of 40 billion nodes. **FedGraph** sends fewer than 80M messages for the same graph. This experiment shows that **FedGraph** has good scalability for very large graphs.

8 RELATED WORK

We categorize the related work as follows.

Graph pattern matching. There have been a large number of algorithms developed for graph pattern matching thus far; these algorithms can generally be classified into backtracking [12, 19, 20, 50], encoding and indexing [5, 23, 46, 57], and decomposition [6, 49]. The first category of algorithm started with [50] and was followed by [12]. An approach of rewriting the query into a neighborhood equivalence class (NEC) tree in terms of neighborhood equivalence is proposed in [20]; dynamic programming is exploited to determine the matching order according to a directed acyclic graph (DAG) established from the pattern in [19]. Backtracking-based subgraph ENUMeration (BENU) [54] divides a subgraph enumeration task into a group of local search tasks that can be executed in parallel, each of which follows a backtracking-based execution plan. In the second category, the labels of a node within a radius are encoded as signatures in [23]. The neighbors or degrees of each node are encoded as indices in [46]. **Match** is an ontology-based index proposed for subgraph matching [57]. Recently, to find the candidates for every edge of the query trees, an index using a compact embedding cluster was proposed in [5]. In the third category, the pattern is decomposed into a series of tree-like subgraphs in [49] and a dense subgraph along with a forest in [6]. The same approaches have been proposed for distributed subgraph matching [3, 4, 31–33].

Federated RDF query. A number of algorithms have been developed for federated RDF query processing, classified into metadata-based queries [2, 17, 21, 42, 44] and ask queries [45]. Due to the autonomy of RDF sources, the major differences among existing algorithms are query decomposition and source selection. In the first category, a vocabulary of interlinked dataset-based OWL language is used as the metadata in [17], and a variant of the R-tree where its leaf nodes store a set of source identifiers is used in [21, 42]. [2] generates the query plan dynamically, considering both data availability and runtime conditions. Recently, a set of capabilities that can map the properties to corresponding subjects and objects were defined and used in [44]. In the second category, ask queries for every triple pattern are sent to the RDF sources and the patterns are annotated with relevant sources

according to the answers in [45]. [9] is the first to consider heterogeneous securities for federated databases and proposed related efficient query processing algorithms.

Ontology-based query processing. Ontological information has been studied and used for keyword queries [24, 30, 36, 37], pattern mining [8] and semantic queries [11, 34, 57]. In the first category, an ontology-based multifaceted search paradigm that links keyword queries to a number of entities in multidistinct ontology views is explored in [37]. In the second category, an approach [8] of mining frequent patterns over graphs uses generalized labels in input taxonomies. In the third category, class hierarchy is exploited in [11] to evaluate queries specified by SPARQL and OWL on RDF graphs, in which distance metrics identify approximate results. Template graph searching is extended by interpolating ontologies to data graphs in [34, 36]. Moreover, [57] leverages the ontology graph to develop filtering strategies to identify semantically related matches.

FedGraph is designed for a brand new graph computation scenario, namely, graph federation. It differs from all the prior works in the following ways. (1) Rather than exact graph pattern matching using identical labels, this work identifies the matches semantically close to the query graph through ontology from distributed graph sources via a mediator in the graph federation. (2) This work proposes a machine learning-based solution for integrating graphs and ontologies that has wider applications than RDF graphs and OWL languages, where common uniform resource identifiers (URIs) often need manual identification. (3) This work aims to propose a general framework for graph federation that is more suitable to be formulated by a graph model. Compared to the RDF, the graph-based model has the advantage of identifying instances of a relationship of the same type [27]. In other words, the RDF-based model is not suitable for performing subgraph matching, which is one of the critical features in graph federation. (4) The graph federation is autonomous and heterogeneous, which is not considered in prior works, e.g., logical and physical scheduling algorithms. The experiments show that these algorithms can very efficiently process subgraph matching, e.g., 53 times faster than the SPARQL-based solution.

9 CONCLUSION

We made the first attempt to study query answering in graph federation by incorporating the features of autonomy and heterogeneity. We abstracted these features, formalized the subgraph matching problem in graph federation, studied its complexity, and developed approximate algorithms for generating distributed query plans. We proposed machine learning techniques to identify common entities (resp. concepts) between different graphs (resp. ontologies). Our experimental study showed that this framework is promising for reducing communication costs and minimizing execution time. In future work, we will study the challenges incurred by graph federation dynamic and private features. Additionally, we will extend the techniques to other types of graph queries in graph federation.

REFERENCES

- [1] 2020. The Linked Open Data Cloud. <https://lod-cloud.net/>.
- [2] Maribel Acosta, Maria-Esther Vidal, Tomas Lampo, Julio Castilho, and Edna Ruckhaus. 2011. ANAPSID: an adaptive query processing engine for SPARQL endpoints. In *ISWC*. 18–34.
- [3] Foto N Afrati, Dimitris Fotakis, and Jeffrey D Ullman. 2013. Enumerating subgraph instances using map-reduce. In *ICDE*. IEEE, 62–73.
- [4] Khaled Ammar, Frank McSherry, Semih Salihoglu, and Manas Joglekar. 2018. Distributed Evaluation of Subgraph Queries Using Worst-case Optimal and Low-Memory Dataflows. *Proc. VLDB Endow.* 11, 6 (2018), 691–704.
- [5] Bibek Bhattarai, Hang Liu, and H Howie Huang. 2019. Ceci: Compact embedding cluster index for scalable subgraph matching. In *SIGMOD*. 1447–1462.
- [6] Fei Bi, Lijun Chang, Xuemin Lin, Lu Qin, and Wenjie Zhang. 2016. Efficient subgraph matching by postponing cartesian products. In *SIGMOD*. 1199–1214.
- [7] David C. Blair. 1979. Information Retrieval, 2nd ed. C.J. Van Rijsbergen. London: Butterworths. *Journal of the American Society for Information Science* 30, 6 (1979), 374–375.
- [8] Ali Cakmak and Gultekin Ozsoyoglu. 2008. Taxonomy-superimposed graph mining. In *EDBT*. 217–228.
- [9] Yang Cao, Wenfei Fan, Yanghao Wang, and Ke Yi. 2020. Querying shared data with security heterogeneity. In *Proceedings of the 2020 ACM SIGMOD International Conference on Management of Data*. 575–585.
- [10] Daniel Cer, Yinfei Yang, Sheng-yi Kong, Nan Hua, Nicole Limtiao, Rhomni St. John, Noah Constant, Mario Guajardo-Cespedes, Steve Yuan, Chris Tar, Brian Strope, and Ray Kurzweil. 2018. Universal Sentence Encoder for English. In *EMNLP*. 169–174.
- [11] Olivier Corby, Rose Dieng-Kuntz, Fabien Gandon, and Catherine Faron-Zucker. 2006. Searching the semantic web: Approximate query processing based on ontologies. *IEEE Intelligent Systems* 21, 1 (2006), 20–27.
- [12] L. P. Cordella, P. Foggia, C. Sansone, and M. Vento. 2004. A (sub)graph isomorphism algorithm for matching large graphs. *IEEE Trans. Pattern Anal. Mach. Intell.* 26, 10 (2004), 1367–1372.
- [13] Jacob Devlin, Ming-Wei Chang, Kenton Lee, and Kristina Toutanova. 2018. BERT: Pre-training of Deep Bidirectional Transformers for Language Understanding. *CoRR* (2018).
- [14] Kemele M Endris, Philipp D Rohde, Maria-Esther Vidal, and Sören Auer. 2019. Ontario: Federated query processing against a semantic data lake. In *DEXA*. 379–395.
- [15] Hector Garcia-Molina, Jeffrey D Ullman, and Jennifer Widom. 2000. *Database system implementation*. Vol. 654. Prentice Hall Englewood Cliffs.
- [16] Michael R. Garey and David S. Johnson. 1979. *Computers and intractability: a guide to the theory of NP-completeness*. W.H. Freeman.
- [17] Olaf Görlitz and Steffen Staab. 2011. Splendid: Sparql endpoint federation exploiting void descriptions. In *COLD*. EUR-WS.org, 13–24.
- [18] Glen L Gray and Roger S Debreceeny. 2014. A taxonomy to guide research on the application of data mining to fraud detection in financial statement audits. *International Journal of Accounting Information Systems* 15, 4 (2014), 357–380.
- [19] Myoungji Han, Hyunjoon Kim, Geonmo Gu, Kunsu Park, and Wook-Shin Han. 2019. Efficient subgraph matching: Harmonizing dynamic programming, adaptive matching order, and failing set together. In *SIGMOD*. 1429–1446.
- [20] Wook-Shin Han, Jinsoo Lee, and Jeong-Hoon Lee. 2013. Turboiso: towards ultrafast and robust subgraph isomorphism search in large graph databases. In *SIGMOD*. 337–348.
- [21] Andreas Harth, Katja Hose, Marcel Karnstedt, Axel Polleres, Kai-Uwe Sattler, and Jürgen Umbrich. 2010. Data summaries for on-demand queries over linked data. In *WWW*. 411–420.
- [22] Waqar Hasan and Rajeev Motwani. 1994. Optimization Algorithms for Exploiting the Parallelism-Communication Tradeoff in Pipelined Parallelism. In *VLDB*. 36–47.
- [23] Huahai He and Ambuj K Singh. 2008. Graphs-at-a-time: query language and access methods for graph databases. In *SIGMOD*. 405–418.
- [24] Hanh Huu Hoang and A Min Tjoa. 2006. *The state of the art of ontology-based query systems: A comparison of existing approaches*. Citeseer.
- [25] Dorit S Hochba. 1997. Approximation algorithms for NP-hard problems. *ACM Sigact News* 28, 2 (1997), 40–52.
- [26] Johannes Hoffart, Fabian M Suchanek, Klaus Berberich, and Gerhard Weikum. 2013. YAGO2: A spatially and temporally enhanced knowledge base from Wikipedia. *Artificial Intelligence* 194 (2013), 28–61.
- [27] <https://neo4j.com/blog/rdf-triple-store-vs-labeled-property-graph-difference/>. [n.d.]. ([n.d.]).
- [28] Yannis E. Ioannidis and Younkung Cha Kang. 1991. Left-Deep vs. Bushy Trees: An Analysis of Strategy Spaces and its Implications for Query Optimization. In *SIGMOD*. 168–177.
- [29] Ryan Kiros, Yukun Zhu, Ruslan Salakhutdinov, Richard S. Zemel, Raquel Urtasun, Antonio Torralba, and Sanja Fidler. 2015. Skip-Thought Vectors. In *Advances in Neural Information Processing Systems*. 3294–3302.
- [30] Rasmus Knappe, Henrik Bulskov, and Troels Andreasen. 2007. Perspectives on ontology-based querying. *International Journal of Intelligent Systems* 22, 7 (2007), 739–761.
- [31] Longbin Lai, Lu Qin, Xuemin Lin, and Lijun Chang. 2015. Scalable Subgraph Enumeration in MapReduce. *Proc. VLDB Endow.* 8, 10 (2015), 974–985.
- [32] Longbin Lai, Lu Qin, Xuemin Lin, Ying Zhang, and Lijun Chang. 2016. Scalable Distributed Subgraph Enumeration. *Proc. VLDB Endow.* 10, 3 (2016), 217–228.
- [33] Longbin Lai, Zhu Qing, Zhengyi Yang, Xin Jin, Zhengmin Lai, Ran Wang, Kongzhang Hao, Xuemin Lin, Lu Qin, Wenjie Zhang, Ying Zhang, Zhengping Qian, and Jingren Zhou. 2019. Distributed Subgraph Matching on Timely Dataflow. *Proc. VLDB Endow.* 12, 10 (2019), 1099–1112.
- [34] Eric Little, Kedar Sambhoo, and James Llinas. 2008. Enhancing graph matching techniques with ontologies. In *FUSION*. 1–8.
- [35] Yu Liu, Yong Li, Yong Niu, and Depeng Jin. 2020. Joint Optimization of Path Planning and Resource Allocation in Mobile Edge Computing. *Trans. Mob. Comput.* (2020), 2129–2144.
- [36] Hanchao Ma, Morteza Alipour Langouri, Yinghui Wu, Fei Chiang, and Jiaying Pi. 2019. Ontology-based Entity Matching in Attributed Graphs. *VLDB* 12, 10 (2019), 1195–1207.
- [37] Eetu Mäkelä, Eero Hyvönen, and Sampsa Saarela. 2006. Ontogator semantic view-based search engine service for web applications. In *ISWC*. 847–860.
- [38] Grzegorz Malewicz, Matthew H Austern, Aart JC Bik, James C Dehnert, Ilan Horn, Naty Leiser, and Grzegorz Czajkowski. 2010. Pregel: a system for large-scale graph processing. In *SIGMOD*. 135–146.
- [39] Fatemeh Nargesian, Erkang Zhu, Renée J. Miller, Ken Q. Pu, and Patricia C. Arocena. 2019. Data Lake Management: Challenges and Opportunities. *Proc. VLDB Endow.* 12, 12 (2019), 1986C1989.
- [40] Xiaofeng Ouyang, Liang Hong, and Lujia Zhang. 2018. Query Associations Over Big Financial Knowledge Graph. In *BigSDM*. 199–211.
- [41] Peng Peng, Lei Zou, M. Tamer Ozsu, Lei Chen, and Dongyan Zhao. 2016. Processing SPARQL queries over distributed RDF graphs. *The VLDB journal* 25, 2 (2016), 243–268.
- [42] Fabian Prasser, Alfons Kemper, and Klaus A Kuhn. 2012. Efficient distributed query processing for autonomous RDF databases. In *EDBT*. 372–383.
- [43] Miao Qiao, Hao Zhang, and Hong Cheng. 2017. Subgraph Matching: on Compression and Computation. *Proc. VLDB Endow.* 11, 2 (2017), 176–188.
- [44] Muhammad Saleem and Axel-Cyrille Ngonga Ngomo. 2014. Hibiscus: Hypergraph-based source selection for sparql endpoint federation. In *European semantic web conference*. Springer, 176–191.
- [45] Andreas Schwarte, Peter Haase, Katja Hose, Ralf Schenkel, and Michael Schmidt. 2011. Fedx: Optimization techniques for federated query processing on linked data. In *ISWC*. 601–616.
- [46] Haichuan Shang, Ying Zhang, Xuemin Lin, and Jeffrey Xu Yu. 2008. Taming verification hardness: an efficient algorithm for testing subgraph isomorphism. *Proceedings of the VLDB Endowment* 1, 1 (2008), 364–375.
- [47] Patrick Stükel, Ole von Bargaen, Adrian Rutle, and Yngve Lamo. 2020. GraphQL Federation: A Model-Based Approach. (2020).
- [48] Shixuan Sun and Qiong Luo. 2019. Scaling Up Subgraph Query Processing with Efficient Subgraph Matching. In *ICDE*. IEEE, 220–231.
- [49] Zhao Sun, Hongzhi Wang, Haixun Wang, Bin Shao, and Jianzhong Li. 2012. Efficient Subgraph Matching on Billion Node Graphs. *VLDB* 5, 9 (2012), 788–799.

- [50] Julian R Ullmann. 1976. An algorithm for subgraph isomorphism. *Journal of the ACM (JACM)* 23, 1 (1976), 31–42.
- [51] Vijay V. Vazirani. 2001. *Approximation algorithms*. Springer.
- [52] Chihping Wang and Ming-Syan Chen. 1996. On the complexity of distributed query optimization. *IEEE Transactions on Knowledge and Data Engineering* 8, 4 (1996), 650–662.
- [53] Haixun Wang, Hao He, Jun Yang, Philip S Yu, and Jeffrey Xu Yu. 2006. Dual labeling: Answering graph reachability queries in constant time. In *ICDE*. IEEE, 75–75.
- [54] Zhaokang Wang, Rong Gu, Weiwei Hu, Chunfeng Yuan, and Yihua Huang. 2019. BENU: Distributed Subgraph Enumeration with Backtracking-Based Framework. In *ICDE*. IEEE, 136–147.
- [55] Hao Wei, Jeffrey Xu Yu, Can Lu, and Xuemin Lin. 2016. Speedup graph processing by graph ordering. In *Proceedings of the 2016 International Conference on Management of Data*. 1813–1828.
- [56] Wentao Wu, Hongsong Li, Haixun Wang, and Kenny Qili Zhu. 2012. Probase: a probabilistic taxonomy for text understanding. In *SIGMOD*. 481–492.
- [57] Yinghui Wu, Shengqi Yang, and Xifeng Yan. 2013. Ontology-based subgraph querying. In *ICDE*. 697–708.
- [58] Fanjin Zhang, Xiao Liu, Jie Tang, Yuxiao Dong, Peiran Yao, Jie Zhang, Xiaotao Gu, Yan Wang, Bin Shao, Rui Li, et al. 2019. OAG: Toward linking large-scale heterogeneous entity graphs. In *Proceedings of the 25th ACM SIGKDD*. 2585–2595.
- [59] Amal Zouaq and Felix Martel. 2020. What is the schema of your knowledge graph? leveraging knowledge graph embeddings and clustering for expressive taxonomy learning. In *Proceedings of The International Workshop on Semantic Big Data*. 1–6.